

## A hybrid evolutionary algorithm for secure multi-objective distribution feeder reconfiguration

Ali Azizivahed<sup>a</sup>, Hossein Narimani<sup>b</sup>, Ehsan Naderi<sup>c</sup>, Mehdi Fathi<sup>b</sup>, Mohammad Rasoul Narimani<sup>d,\*</sup>

<sup>a</sup> Department of Electrical Engineering, Shiraz University of Technology, Shiraz, Iran

<sup>b</sup> Department of Electrical Engineering, Kermanshah Branch, Islamic Azad University, Kermanshah, Iran

<sup>c</sup> Faculty of Engineering and Technology, Razi University, Eslam Abad Gharb, Kermanshah, Iran

<sup>d</sup> Electrical and Computer Engineering, Missouri University of Science and Technology, Rolla, USA

### ARTICLE INFO

*Article history:*

Received 11 December 2016

Received in revised form

12 June 2017

Accepted 14 July 2017

Available online 17 July 2017

*Keywords:*

Distribution feeder reconfiguration (DFR)

Distributed generation (DG)

Mutation operator

Evolutionary algorithm

Voltage stability index (VSI)

### ABSTRACT

Distribution Feeder Reconfiguration (DFR) is an important technique to improve the performance of distribution networks. The common objectives considered in the DFR problem are power loss and voltage deviation which are important objectives for traditional distribution systems. Security issues caused by Distributed Generations (DGs) in modern distribution systems which can potentially jeopardize power system security has almost neglected in power system operation problem. Toward this end, this study considers the power loss, Voltage Stability Index (VSI), and number of switching as objective functions which can satisfy both operation and security expectations. The Backward-Forward Sweep (BFS) method known for easy convergence has been employed for power flow calculations. Because of the increase in DG penetration in distributed systems, the impacts of these units are investigated. A powerful optimization algorithm based on hybridization of Shuffled Frog Leaping Algorithm (SFLA) and Particle Swarm Optimization (PSO) is proposed to solve the proposed problem. The proposed algorithm is a combination of strong mutation operator, original SFLA and original PSO algorithms which has high population diversity and search ability. The proposed algorithm has been applied to a complex multi-modal benchmark function and also two different distribution networks including 33- and 95-bus test systems.

© 2017 Elsevier Ltd. All rights reserved.

### 1. Introduction

The concept of reconfiguration process is modifying the structure of distribution feeders in order to optimize certain objective functions subject to satisfy a set of constraints and limitations [1]. Generally, the Distribution Feeder Reconfiguration (DFR) is carried out by managing the states of tie-switches and sectionalizes components in a distribution feeder without removing the section of the system as an island. Because of the inherit characteristic of the DFR problem such as having discontinuous variables and etc., the Mathematical-based optimization algorithms are not proper candidate to solve this problem. Toward this end, special attentions

have been paid to heuristic algorithms to solve the DFR problem. Advantages of heuristic algorithms in solving the optimization problem make these algorithms popular candidate to solve optimization problems. Therefore proposing more efficient algorithm has become an ongoing research topic.

The power loss and voltage deviation objectives are further studied by researchers in solving the DFR problem in conventional form [2]. But, investigation the conventional DFR problem cannot take care of other issues in the distribution systems. Therefore the results of conventional DFR are not acceptable in modern distribution systems where the penetration of Distributed Generations (DGs) is being increased and the system suffers from security issues.

Recently, the share of DG resources in distribution networks has been rapidly increased [2]. The increasing utilization of these resources is due to their characteristics such as closing to load points, small-scale, reducing the active power transmission loss and etc. Although there is a vast body of research on the DFR problem

\* Corresponding author.

E-mail addresses: [A.Azizi@sutech.ac.ir](mailto:A.Azizi@sutech.ac.ir) (A. Azizivahed), [Hosein.Narimani83@gmail.com](mailto:Hosein.Narimani83@gmail.com) (H. Narimani), [E.Naderi@stu.razi.ac.ir](mailto:E.Naderi@stu.razi.ac.ir) (E. Naderi), [FathiMahdi83@gmail.com](mailto:FathiMahdi83@gmail.com) (M. Fathi), [Mn9t5@mst.edu](mailto:Mn9t5@mst.edu) (M.R. Narimani).

without consideration of DGs effect, little attention has been paid to the consideration of DGs influence on DFR problem. Beside several benefits that DGs have brought to distribution systems, they can jeopardize the stability of distribution systems by decreasing the short circuit level. This issue is corresponding to the operation and design of the distribution networks. Also, the Short Circuit Current (SCC) level is directly proportional to the sub-station voltage. The SCC can be increased by reconfiguring the structure of distribution system. To this end, the security issues caused by DG implementation are taken into account beside the conventional objective function and constraints. It is notable that considering the security issues in the proposed DFR modeling and formulation makes the proposed study more practical from operation and planning point of views.

Another important objective in operation of distribution system, which this study focuses on, is reducing the number of switching operations which can have negative effect on the overall operation cost of network. It is necessary to note that number of switching is usually ignored or not considered simultaneously with other objectives. The substantial decreasing in the number of switching leads to the reduction of operation and maintenance cost.

Considering security objectives and switching cost along with the traditional objective function necessitate the optimization problem to be solved as a Multi-Objective Optimization Problem (MOOP). In other words, evaluating the DFR problem as a MOOP covers different aspects and needs a tool to optimize all objective simultaneously. Toward this end Pareto-based approach, which can obtain a set of optimal solutions instead of one, is employed in which enables the power system operators to select one of these solutions based on their desires. Furthermore, a fuzzy decision making is utilized to find the best compromise solution. To verify the suitability of the presented algorithm it is applied to 33- and 95-bus test systems. Simulation results prove the ability of the proposed algorithm in solving the proposed optimization problem.

During the years, different numerical algorithms have been utilized to solve the network reconfiguration problem such as, distance measurement method [3], brute-force solution [4], Integer Programming (IP) [5,6] and G-Net inference mechanism approach [7]. But, these numerical algorithms cannot guarantee to recognize the global optimal solution of DFR problem. On the other side, these optimization algorithms have extra restrictions including continuation and derivability of the objective functions, the discrete inheritance of the switches status and also constraint for radial configuration of distribution feeders. Toward this end, these numerical-based and mathematical algorithms are not suitable candidate for solving the DFR and more specifically MODFR problems. Recently many heuristic and meta-heuristic algorithms have been introduced to ameliorate these restrictions.

A literature survey manifest that, various evolutionary-based optimization algorithms have been utilized to solve the different forms of the network reconfigurations.

Particle Swarm Optimization (PSO) algorithm for solving the DFR problem was implemented in Ref. [8]. In Ref. [9], a hybrid approach based on Discrete PSO (DPSO) and Honey Bee Mating Optimization (HBMO) was presented to solve Multi-Objective DFR (MODFR) problem. A Guaranteed Convergence PSO (GCPSO) algorithm for solving the DFR problem was proposed in Ref. [10]. A Multi-objective HBMO (MHBMO) algorithm was employed to solve the DFR problem in Ref. [11]. A combination of Bacterial Foraging Algorithm (BFA) and Nelder-Mead (NM) method was used to solve DFR with phase balancing restriction in Ref. [12]. A New Fuzzy Adaptive PSO (NFAPSO) algorithm was employed in Ref. [13] to evaluate the DFR problem. Teacher Learning Algorithm (TLA) was proposed in Ref. [14] to solve the Stochastic DFR (SDFR) problem considering Fuel Cell Power Plants (FCPP) and Probabilistic Load

Flow (PLF) based on Point Estimate Method (PEM). In Ref. [15], an Adaptive Modified PSO (AMPSO) was presented to solve the DFR problem considering Wind Power Plant (WPP). A Multi-objective modified HBMO (MHBMO) algorithm was presented in Ref. [16] to solve the DFR problem considering renewable energy resources. A probabilistic approach based on the Genetic Algorithm (GA) for solving the DFR problem was proposed in Ref. [17]. An Improved Shuffled Frog Leaping Algorithm (ISFLA) was introduced in Ref. [18] to solve the MODFR problem for reliable operation of distribution system. An Interval Multi-Objective Evolutionary Algorithm (IMOEA) was presented in Ref. [19] to solve the DFR problem. A new Self Adaptive Modified Bat Algorithm (SAMBA) and Teacher Learning Optimization (SMTLO) were introduced in Refs. [20,21], respectively to solve the DFR problem from reliability and probabilistic points of view.

Ref. [22] presented a Multi-Objective Invasive Weed Optimization (MOIWO) algorithm for solving Optimal Network Reconfiguration (ONR) problem in radial distribution systems. In Ref. [23] a Quantum PSO (QPSO) algorithm was presented to solve the DFR problem in distribution system equipped with DG units. A GA algorithm was utilized in Ref. [24] for solving the DFR problem considering DG resources and hourly Locational Marginal Prices (LMPs) of wholesale market. A  $\theta$ -Modified Bat Algorithm was introduced in Ref. [25] to solve the DFR problem in a stochastic framework. In Ref. [26], a Social Spider Optimization (SSO) algorithm was proposed to solve the DFR problem considering Plug-in Electric Vehicles (PEVs) and Vehicle-to-Grid (V2G). A heuristic approach according to Uniform Voltage Distribution Algorithm (UVDA) based constructive reconfiguration was proposed in Ref. [27] to solve the optimal allocation and sizing of DG units by DFR. A Multi-objective Hybrid Big Bang-Big Crunch (MOHBB-BC) algorithm was presented in Refs. [28,29] for solving the multi-objective optimal DFR problem in distribution networks while DG allocation and load uncertainty were considered in Ref. [28] and capacitor placement was taken into account in Ref. [29] and finally, a comprehensive review on network reconfiguration in distribution systems to decrease the power loss and improve the system reliability was presented in Ref. [30].

A general outline of these references has been organized and presented in Table 1 to ease the access of essential information of the researches such as merits, demerits and etc.

According to Table 1, only one of the presented studies considers the security objective i.e. the voltage stability in DFR problem. Also, most of them neglected the switching cost which can play an important role in decreasing the operation and maintenance cost in distribution systems. Toward this end, the suitability of the proposed approach in this study for solving different versions of DFR problems is much more require. In this regard, the contribution of this study is twofold which are related to the presented evolutionary algorithm and the considered objective functions.

Solving the MODFR problem requires an accurate and powerful optimization algorithm especially in DG resources included distribution system. To this end, a novel Hybrid Modified Shuffled Frog Leaping Algorithm-Particle Swarm Optimization (HMSFLA-PSO) is proposed to cope with the complexities of the proposed DFR problem. The original PSO and SFLA algorithms have few drawbacks such as; (1) premature converge or trapped into local optimal and (2) converge to global optimal in a long period of time. Toward this end, an appropriate and strong strategy of mutation operator is added to the hybrid algorithm to increase the diversity of population and search ability of the algorithm.

Moreover, three different objective functions including power loss, Voltage Stability Index (VSI) and number of switching are considered in this study. Also, Backward-Forward Sweep (BFS) algorithm has been employed for the load flow analysis. This BFS

**Table 1**  
Overview of the presented references to solve the different forms of DFR problem.

Ref.	Algorithm	Objective functions						Remark			
		Cost	PL	VDI	VSI	NOS	FLB	PBI	PE	CLI	
[1]	EGSA	✓	✓								1. ENS is considered as third objective function for reliability assessment. 2. Pareto-optimal method is implemented to handle the MOOP. 3. Test systems are including 33-bus and 70-bus distribution systems.
[2]	EGSA	✓	✓								1. Improving the transient stability is considered as an objective function. 2. Pareto-optimal method is implemented to handle the MOOP. 3. The effects of DGs are considered in problem formulation. 4. Simulations and programming are performed with DigSILENT® power factory software. 5. Test system is 33-bus distribution network.
[8]	PSO	✓		✓							1. Weight factor method is used to handle the MOOP. 2. Test system is 31-node distribution system with three feeders and four tie switches.
[9]	Hybrid DPSO and HBMO	✓	✓		✓	✓					1. Weight factor method is used to handle the MOOP. 2. Test systems are including 32-bus and 70-bus distribution systems.
[10]	GCPSO	✓	✓								1. Weight factor method is used to handle the MOOP. 2. Test systems are including 16-bus, 33-bus and 129-bus distribution systems.
[11]	MHBMO	✓	✓			✓					1. Weight factor method is used to handle the MOOP. 2. Test systems are including 32-bus and 86-bus distribution systems.
[12]	Hybrid BFA and NM	✓				✓					1. Weight factor method is used to handle the MOOP. 2. Test system is IEEE 123-bus test network.
[13]	NFAPSO	✓									1. FADPSO and FABPSO algorithms are implemented to solve the problem. 2. Test systems are including 32-bus and 86-bus distribution systems.
[14]	TLA	✓	✓				✓				1. Stochastic model of DFR problem is solved. 2. Fuzzy decision making method is utilized to handle the MOOP. 3. Test system is 86-bus TCP distribution system considering FCPPs.
[15]	AMPSO	✓	✓	✓							1. Fuzzy satisfying method is utilized to handle the MOOP. 2. Scenario-based MODFR is solved. 3. Wind power is integrated to the model. 4. Test systems are including 32-bus and 69-bus distribution systems.
[16]	MHBMO	✓	✓	✓							1. Pareto-optimal method is implemented to handle the MOOP. 2. The effects of fuel cell, wind energy and photovoltaic power are considered. 3. Test system is 32-bus distribution network considering renewable energy sources.
[17]	GA				✓						1. Probabilistic model of DFR problem is solved. 2. Test systems are including 16-bus and 33-bus distribution systems.
[18]	ISFLA		✓								1. Reliability objectives are considered too, such as SAIFI, SAIDI and AENS. 2. Pareto-optimal method is implemented to handle the MOOP.
[19]	IMOEA	✓	✓		✓		✓				1. Weight factor method is used to handle the MOOP. 2. Test system is 70-node distribution network.
[20]	SAMBA		✓								1. Reliability objectives such as AENS and SAIFI are considered. 2. Pareto-optimal method is implemented to handle the MOOP. 3. Stochastic model of MODFR problem is solved considering wind power uncertainties. 4. Test system is 32-bus distribution network.
[21]	SAMTLO	✓	✓	✓			✓				1. Probabilistic model of MODFR is solved. 2. Fuzzy decision making and Pareto-optimal methods are utilized to handle the MOOP. 3. Uncertainty of wind power is considered. 4. Test systems are including 32-bus and 86-bus distribution systems.
[22]	MOIWO		✓	✓		✓	✓				1. Pareto-optimal method is implemented to handle the MOOP. 2. Test systems are including IEEE 33-bus distribution network and 84-bus Taiwan power company.
[23]	QPSO			✓							1. Different models of DG units were considered. 2. Test systems are including IEEE 33-bus and PG&E 69-bus distribution systems.
[24]	GA		✓								1. Market-based method is presented to solve the DFR problem. 2. LMP and effects of DG units are considered. 3. Test systems are including 16-bus and 204-bus distribution systems.
[25]	θ-Modified Bat Algorithm		✓	✓							1. Stochastic model of MODFR is solved. 2. Proposed algorithm is integrated with cloud theory to handle the uncertainties. 3. Reliability objectives such as SAIFI and SAIDI are considered.
[26]	SSO		✓								4. Test systems are including IEEE 32-bus and 69-bus distribution systems.
[27]	UVDA			✓							1. The effects of PEV and V2G are considered in the problem formulation. 2. Test system is IEEE 69-bus distribution network.
[28]	MOHBB-BC		✓	✓	✓		✓				1. DG allocation and sizing are considered. 2. Test systems are including 33-bus and 69-bus distribution systems. 1. DG allocation is considered along with DFR problem. 2. Pareto-optimal method is implemented to handle the MOOP. 3. Load uncertainty is considered.
[29]	MOHBB-BC		✓	✓		✓					4. Test systems are including 25-bus and 33-bus distribution systems. 1. Capacitor placement is considered along with DFR problem. 2. Fuzzy-based combination of objective functions is utilized. 3. Test systems are including 25-bus, 33-bus and 94-bus distribution systems.

PL, Power Loss; VDI, Voltage Deviation Index; VSI, Voltage Stability Index; NOS, Number of Switching; FLB, Feeder Load Balancing; PBI, Phase Balancing Index; PE, Pollution Emission; CLI, Current Loading Index.

method utilizes complete advantage of ladder structure of distribution network, to achieve high speed, robust convergence, low memory requirements and does not need any Jacobian matrix.

In the proposed MOOP, obtains a set of optimal solutions instead of one because the considered objectives are not in line with each other. This is done by utilizing a repository to save all non-dominated solutions (Pareto-optimal solutions) at each iterate. Also, a fuzzy decision making strategy is used for sorting all Pareto-optimal solutions based on their importance.

Finally, three different criterions are implemented to analyze the obtained Pareto-optimal solutions. These criterions include Generational Distance (GD), Spacing Parameter (SP) and Diversity Metric (DM). The proposed approach is simple, easy to implement and also high computationally efficient. Yet another it has a stable operation for solving the DFR and MODFR problems in which the obtained outcomes approve this statement.

In this regard, the highlighting characteristic features of this study are outlined as follows;

- The MODFR is modeled considering three different objective functions including power loss, Voltage Stability Index (VSI) and, number of switching.
- Utilizing the Backward-Forward Sweep (BFS) procedure for power flow calculations without considering Jacobian matrix.
- Considering the stability objective function based on the short circuit capacity.
- Presenting a novel and powerful hybrid algorithm, HMSFLA-PSO, for solving the MODFR problem.
- Introducing the robust and strong mutation operator to improve the algorithm performance.
- Considering the effect of DG resources in different aspects.

The remaining of this paper is conducted as follows;

Section 2 presents DFR problem formulation. Multi-objective solution methodology is provided in detail in section 3. The comprehensive descriptions of the proposed approach are developed in section 4. Section 5 presents case studies and numerical results and finally, section 6 concludes the paper.

## 2. Problem formulation

Three different objective functions along with several constraints are needed to implement the proposed DFR problem. All these functions and constraints are introduced and explained in this section.

### 2.1. Desired objective functions

#### 2.1.1. Power loss

The active power loss can be modeled as follows [31]:

$$f_1 = P_L(X) = \sum_{i=1}^{N_t} R_{t,i} \times (|I_{t,i}|)^2 + \sum_{j=1}^{N_r} R_{r,j} \times (|I_{r,j}|)^2 \quad (1)$$

Where,  $R_{t,i}$  ( $R_{r,j}$ ) and  $I_{t,i}$  ( $I_{r,j}$ ) are resistance and actual current of  $i$ th ( $j$ th) branch (transformer) in the test system, respectively.  $N_t$  ( $N_r$ ) is the number of branches (transformers) in network and,  $P_L$  is the summation of active power loss (MW). Also,  $X$  is the vector of control variables for the proposed DFR problem, which can be presented as follows;

$$X = [TS_1, TS_2, \dots, TS_{N_{TS}}, SW_1, SW_2, \dots, SW_{N_{SW}}, P_1^{DG}, P_2^{DG}, \dots, P_{N_{DG}}^{DG}] \quad (2)$$

Where,  $TS_i$  is the state of the  $i$ th tie switch with zero and one related to open and close states, respectively and  $N_{TS}$  is number of tie switches.  $SW_i$  is  $i$ th sectionalizing switch number which forms a loop along with  $TS_i$  (ith tie switch), and  $N_{SW}$  is the number of sectionalizing switches.  $P_i^{DG}$  is active output power of  $i$ th DG resources and  $N_{DG}$  is the number of DG units.

#### 2.1.2. Voltage stability index

Improving VSI based on SCC in the distribution feeder reconfiguration problem is one of the important targets for the distribution network operators. SCC defined based on Thevenin-equivalent, and the equivalent distribution impedance has important effects on voltage stability [32]. The high value of SCC can be interpreted as the ability of bus for increasing the load. Similarly, the low value of SCC means the bus is weak to adopt more load [33]. According to the Thevenin-equivalent from Fig. 1, the power flow equations [34] can be obtained as (3) & (4). Furthermore, the short circuit current is calculated as (5).

$$P_j = \frac{E_{th,j} \times V_j \times (R_{th,j} \cos \theta - X_{th,j} \sin \theta) - R_{th,j} V_j^2}{R_{th,j}^2 + X_{th,j}^2} \quad (3)$$

$$Q_j = \frac{E_{th,j} \times V_j \times (R_{th,j} \sin \theta + X_{th,j} \cos \theta) - X_{th,j} V_j^2}{R_{th,j}^2 + X_{th,j}^2} \quad (4)$$

$$SCC_j = \frac{E_{th,j}}{\sqrt{R_{th,j}^2 + X_{th,j}^2}} \quad (5)$$

All parameters in (3)–(5) are depicted in Fig. 1, and also the  $V_j$  is the voltage magnitude of bus  $j$ . The relation between SCC and voltage is displayed in Fig. 2.

The SCC line in Fig. 2 introduces the short circuit capacity at load bus. The minimum value of SCC for satisfying the voltage stability can be formulated as follows [35];

$$\text{Minimal } SCC_j = \frac{2 \times (\sqrt{P_j^2 + Q_j^2}) \times (1 + \sin \varphi)}{E_{th,j}} \quad (6)$$

The relation between voltage stability in node and SCC is based on the following statements;

- If  $SCC_j > \text{Minimal } SCC_j$  then voltage of bus  $j$  is stable.
- If  $SCC_j < \text{Minimal } SCC_j$  then voltage of bus  $j$  is unstable.
- If  $SCC_j = \text{Minimal } SCC_j$  then voltage of bus  $j$  is critical stable.

Now, the VSI is formulated as follows;

$$VSI_j = \frac{\text{Minimal } SCC_j}{SCC_j} \quad (7)$$

$$PF = \begin{cases} 0 & \text{if } \forall m, VSI_m \geq 0 \\ \infty & \text{Otherwise} \end{cases} \quad (8)$$

$$f_2 = VSI(X) = \frac{1}{N_B} \sum_{j=1}^{N_B} VSI_j + PF \quad (9)$$

Where,  $VSI_j$  is the index of voltage stability at  $j$ th node.  $VSI$  is the voltage stability objective function and  $N_B$  is the number of system's nodes.  $PF$  is implemented as a penalty factor to eliminate the unstable decision variables during optimization process.

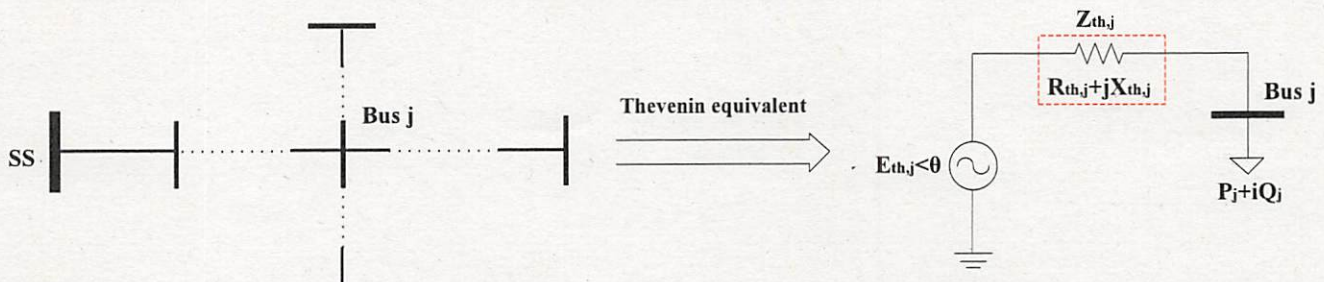


Fig. 1. Thevenin-equivalent of simple distribution system.

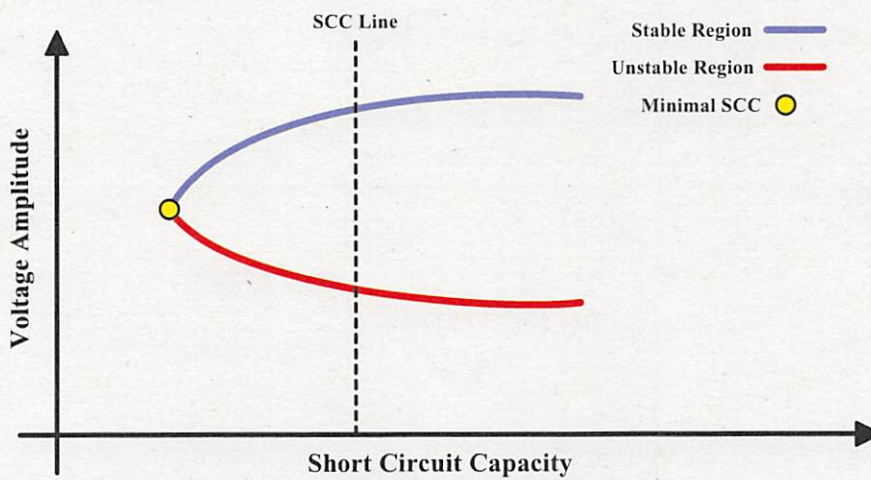


Fig. 2. The SCC-voltage curve.

### 2.1.3. Number of switching

One of the main goals of this study is minimizing the number of switching operation. The number of switching can be represented as follows [11]:

$$f_3 = S(X) = \sum_{i=1}^{N_{sw}} |S_i - S_i^0| \quad (10)$$

Where,  $S_i$  and  $S_i^0$  are the new and old states of  $i$ th tie switch, respectively.  $N_{sw}$  and  $S(X)$  are the number of switches and switching operations, respectively.

### 2.2. Constraints and limitations

#### 2.2.1. Equality constraints

Equality constraint is defined the network structure and can be represented as (11) [36].

$$N_l = N_B - N_{ss} \quad (11)$$

Where,  $N_B$ ,  $N_l$  and  $N_{ss}$  are the number of nodes, branches and substations, respectively.

The above constraint might fail to preserve the radial structure of distribution systems. Toward this end we defined a matrix (Loop-Matrix) in order to generate decision-variables which satisfy the radial structure of the distribution system. Each row of the Loop-Matrix consist the number of branches which corresponds to a separate loop in the distribution network topology. For generating the population, we select only one branch from each row of the

Loop-Matrix. Accordingly, the radial structure of distribution network can be preserved. Furthermore, the Bus incidence matrix has been applied during optimization process in order to check the radially of the system [36].

The bus-incidence matrix ( $A$ ) is a matrix wherein the  $k$ th row of the matrix corresponds to the  $k$ th branch in the network and the  $j$ th column of the matrix corresponds to the  $j$ th bus in the system in which has a branch leaving the bus.

The branch-bus incidence matrix is calculated as follows;

- If the  $k$ th branch (corresponding to  $k$ th row) leaves from  $j$ th bus (corresponding to  $j$ th column) then the matrix element ( $a_{kj}$ ) is equal to 1.
- If the  $k$ th branch (corresponding to  $k$ th row) enters toward  $j$ th bus (corresponding to  $j$ th column) then the matrix element ( $a_{kj}$ ) will be 1.
- All remaining entries will be identically zero.
- While the number of buses is one more than the number of branches in the radial distribution networks, the first column of bus-incidence matrix  $A$  should be deleted to have a square matrix ( $A'$ ).
- If the determinant of branch-bus incidence matrix  $A'$  is 1 or -1, the network's graph will be radial.

#### 2.2.2. Inequality constraints

The inequality constraints are determined by engineering limits on, e.g., the amplitude of voltage, lines flow, transformers and feeder limits which can be presented as follows;

$$V_i^{\min} \leq V_i \leq V_i^{\max} \quad (12)$$

$$|I_{T,i}| \leq I_{T,i}^{\max}, i = 1, 2, \dots, N_T \quad (13)$$

$$|I_{F,i}| \leq I_{F,i}^{\max}, i = 1, 2, \dots, N_F \quad (14)$$

Where,  $V_i$ ,  $V_i^{\min}$  and  $V_i^{\max}$  are voltage magnitude at  $i$ th node and its corresponding minimum and maximum limits, respectively.  $P_{ij}$  and  $P_{ij}^{\max}$  are power flow and maximum limit of power flows over the distribution lines transmitted between nodes  $i$  and  $j$ , respectively.  $I_{T,i}$  and  $I_{T,i}^{\max}$  are the amplitude of the current and its maximum boundary in  $i$ th transformer, respectively.  $I_{F,i}$  and  $I_{F,i}^{\max}$  are the amplitude of current and its maximum boundary in  $i$ th feeder, respectively.  $N_T$  and  $N_F$  are the number of transformers and feeders, respectively.

### 2.2.3. DG resources constraints

In the distribution networks, the role of DG units can be modeled according to PV and PQ nodes [37]. DGs must generate the required reactive power in order to maintain the voltage amplitudes in their allowable boundaries if they are considered as PV model. Both PV and PQ models have been investigated in studies in which each has its own characteristics. The PQ model for these resources is considered for solving the proposed DFR problem.

### 2.3. Power flow algorithm in distribution networks

In the radial distribution networks, there is a unique path from any node in the system to the sub-station and it is one of the important and prominent characteristics of the radial distribution networks. In radial distribution networks, the large R/X ratio causes problems in convergence of conventional load flow algorithms. To this end, this paper employs Backward-Forward Sweep (BFS) method, an effective power flow method for radial distribution systems, for power flow analysis.

The BFS algorithm in general includes two main sub-routines called Backward Sweep (BS) and Forward Sweep (FS). It is worth mentioning that, these two sub-routines are repeated until obtaining an appropriate convergence criterion. The BS is a current or summation of power flows and FS is a computation of voltage drop [38–40]. Table 2 tabulates the sufficient explanation about BFS algorithm and both BS and FS sub-routines.

To have a better demonstration of Table 2 and its relevant calculations, a sample radial distribution feeder with one sub-station as a source is depicted in Fig. 3.

Fig. 3 is suitable for describing the procedure of BFS algorithm in distribution networks. Based on this figure, the explanations of BS and FS sub-routines are as follows:

In the BFS algorithm, initially the voltage amplitude of the last node ( $n$ th node) is supposed to be 1 per unit, then according to branches impedance and the values of load power,  $P_{j-1}$ ,  $Q_{j-1}$  and  $V_{j-1}$  are calculated. In this regard, the obtained values for power in the BS sub-routine can be implemented for computing the output

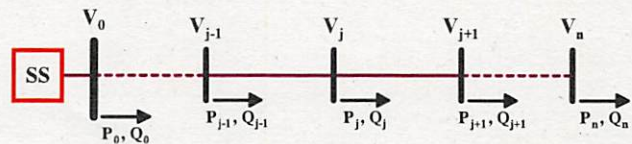


Fig. 3. Single-line diagram of sample radial distribution network.

power of first node. In addition, in the FS sub-routine the value of  $V_{j+1}$  is calculated, this sub-routine must be repeated for sufficient times while an appropriate convergence condition such as  $|V_j^k - V_j^{k-1}| < \epsilon_v$  is obtained.  $\epsilon_v$  is the allowable error for voltage amplitude of nodes and  $k$  is the current iteration.

### 3. Multi-objective solution methodology

Most of the time in the real applications we have to solve a set of objective functions simultaneously as a Multi-Objective Optimization Problem (MOOP). It is notable that, the objective functions may not in line with each other which leads to deal with a set of optimal solutions instead of one. Generally, a sample MOOP can be formulated as follows [41]:

$$\text{Subject to Minimize } f_i(X), i = 1, 2, \dots, N_{OF} \quad (15)$$

$$h_j(X) = 0, j = 1, 2, \dots, H \quad (16)$$

$$g_k(X) \geq 0, k = 1, 2, \dots, K \quad (17)$$

Where,  $f_i(X)$  is  $i$ th objective function.  $h_j(X)$  and  $g_k(X)$  are vectors of equality and inequality constraints, respectively.  $X$  is the decision vector.  $N_{OF}$ ,  $H$  and  $K$  are the number of objective functions, equality and inequality constraints, respectively.

#### 3.1. Process of normalizing the favorable objective functions

The numerical values of different objective functions are not in a same ranges. To this end, it is necessary to bring the values of all objectives in the same range which can be done by normalizing the values of objective functions. Therefore, fuzzy set is considered for each objective function as a value between zero and one. The mathematical model and the figure for a membership function are shown in (18) & (19) and Fig. 4, respectively [42].

$$\mu_i(X) = \begin{cases} 1 & f_i(X) \leq f_i^{\min} \\ \frac{f_i^{\max} - f_i(X)}{f_i^{\max} - f_i^{\min}} & f_i^{\min} \leq f_i(X) \leq f_i^{\max} \\ 0 & f_i(X) \geq f_i^{\max} \end{cases} \quad (18)$$

$$i = 1, 2, \dots, N_{OF} \quad (19)$$

Where,  $\mu_i(X)$  is the fuzzy set for  $i$ th objective function i.e.  $f_i(X)$ .  $f_i^{\min}$ ,  $f_i^{\max}$  and  $N_{OF}$  are the minimum and maximum boundaries of

**Table 2**  
Classification of BS and FS for BFS algorithm in distribution networks.

Sub-routines	Updates	As a function of	Using	According to
BS	Currents or power flows injected into each side	End voltage amplitude	Current or summation of power flows	Zero current or outage of power flows from acceptable range
FS	End voltage amplitude	Currents or power flows injected into each side	Computation of voltage drop	Specification the source voltage

ith objective function and the number of objectives, respectively.

### 3.2. Pareto-optimal solutions and non-dominance concept

One of the best approaches to solve the MOOPs is Pareto-optimal technique. This method acts according to the concept of dominance. The vector  $X_1$  dominants  $X_2$  if the following conditions are satisfied [41]:

$$\forall i \in \{1, 2, \dots, N_{OF}\} \Rightarrow f_i(X_1) \leq f_i(X_2) \quad (20)$$

$$\exists j \in \{1, 2, \dots, N_{OF}\} \Rightarrow f_j(X_1) < f_j(X_2) \quad (21)$$

$$X = [TS_1, TS_2, \dots, TS_{N_{TS}}, SW_1, SW_2, \dots, SW_{N_{SW}}, P_1^{DG}, P_2^{DG}, \dots, P_{N_{DG}}]_{1 \times (N_{TS} + N_{SW} + N_{DG})} \quad (24)$$

### 3.3. Fuzzy decision making engine

In this paper a repository is defined for saving all non-dominated solutions at each iterate. After saving all these solutions, a sorting process is carried out using a decision making strategy. During this process, the Best Compromise Solution (BCS) is opted by selecting the top ranked obtained solutions by applying the following equation [42,43]:

$$N_\mu^j = \frac{\sum_{k=1}^{N_{OF}} (\psi_k \times \mu_{jk})}{\sum_{j=1}^{N_{ND}} \sum_{k=1}^{N_{OF}} (\psi_k \times \mu_{jk})} \quad (22)$$

Where,  $\psi_k$  is the weight factor of  $i$ th objective function and can be opted by the operator based on the importance of objective function.  $N_\mu$  is the compromise solution according to the adjusted weight factors.  $N_{OF}$  and  $N_{ND}$  are the number of objective functions and non-dominated solutions, respectively.

## 4. Proposed approach

### 4.1. Original SFLA

The SFLA was introduced by Eusuff, Lansey and Pasha in 2006 [44]. This algorithm is extracted from social life of frogs when they

are searching their food. In the SFLA, at first the frog population is divided into several memplexes equally. SFLA consists of two searching strategy; the first one is called local search occurs in each memplex, while the second one is exchange the data between memplexes [45]. The following steps should be taken to implement the original SFLA [46]:

**Step 1.** Primary population is generated randomly which is combination of  $N_p$  frogs for the proposed problem based on (23) & (24).

$$P = \begin{bmatrix} X_1 \\ \vdots \\ X_{N_p} \end{bmatrix}_{N_p \times 1} \quad (23)$$

Where,  $P$  and  $N_p$  are the vector and the size of the population, respectively.

It is necessary to note that, after generating the population, the objective function value is computed in which the population is sorted based on.

**Step 2.** The frogs are splitted into  $m$  memplexes in which each memplex includes  $n$  frogs.

**Step 3.** A local search is started and in any memplexes the frogs with the best and the worst fitness are specified and labeled as  $X_B$  and  $X_W$ , respectively. In addition, the frog with best solution in all population is specified as  $X_G$ . The aim of this section is improving the fitness of worst frogs by (25)–(27) which is illustrated in Fig. 5.

$$Dis_i = rand(1, 1)[X_B - X_W] \quad (25)$$

$$X_W^N = X_W^C + Dis_i \quad (26)$$

$$-Dis_{max} \leq Dis_i \leq Dis_{max} \quad (27)$$

Where,  $Dis_i$ ,  $Dis_{min}$  and  $Dis_{max}$  are displacement and allowable

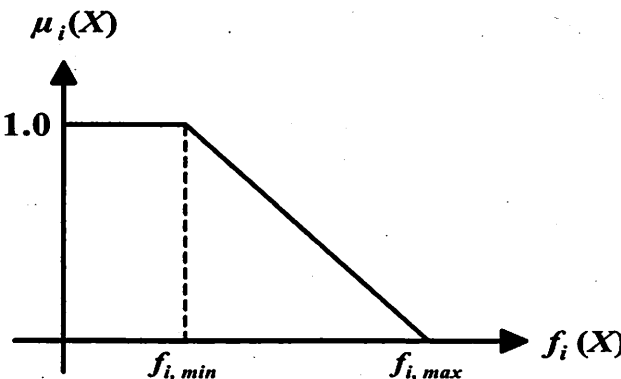


Fig. 4. Trapezoidal membership function for all three objective functions.

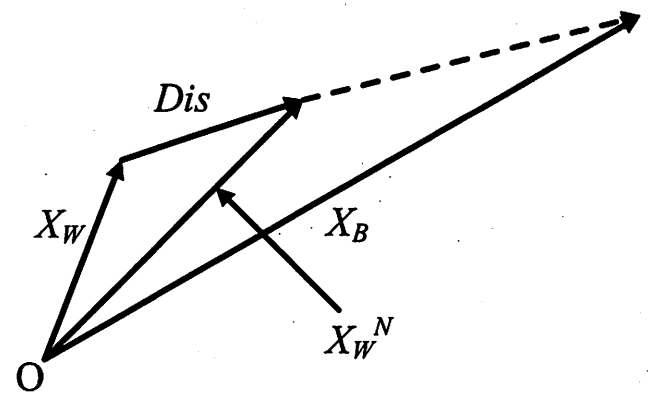


Fig. 5. Movement of worst frog toward best one in SFL algorithm.

minimum and maximum displacement boundaries of  $i^{\text{th}}$  frog, respectively.  $\text{rand}(1, 1)$  is a random number in  $[0 - 1]$ .  $X_W^C$  and  $X_W^N$  are current and new position of the worst frog, respectively.

After using (25) & (26), the previous position of frogs is replaced by new one if new position is improved. It is notable that, these equations are repeated for specific number of iterations namely  $\overline{I\!ter}_{\max}$ . But, if no improvement was obtained, the mentioned process is carried out again using (25) & (26) with the exception that  $X_B$  is replaced by  $X_G$ . In this conditions, if the frogs cannot become better, the new frogs are generated randomly in which  $X_W$  is replaced with.

**Step 4.** After improving the position of frogs, new population are classified from best fitness to the worst ones.

**Step 5.** If reaching to the maximum iteration number or stopping criteria achieved, algorithm stopped, otherwise go back to step 2.

The flowchart of the SFLA is depicted in Fig. 6 for better understanding. It is necessary to note that, two parameters  $I\!ter_{\max}$  and  $\overline{I\!ter}_{\max}$  are maximum number of iterations related to main routine of the proposed algorithm and the local search sub-routine for memplexes, respectively.

#### 4.2. Modified SFLA

The original SFLA has some drawbacks such as converge to local optimal and premature convergence. The premature convergence

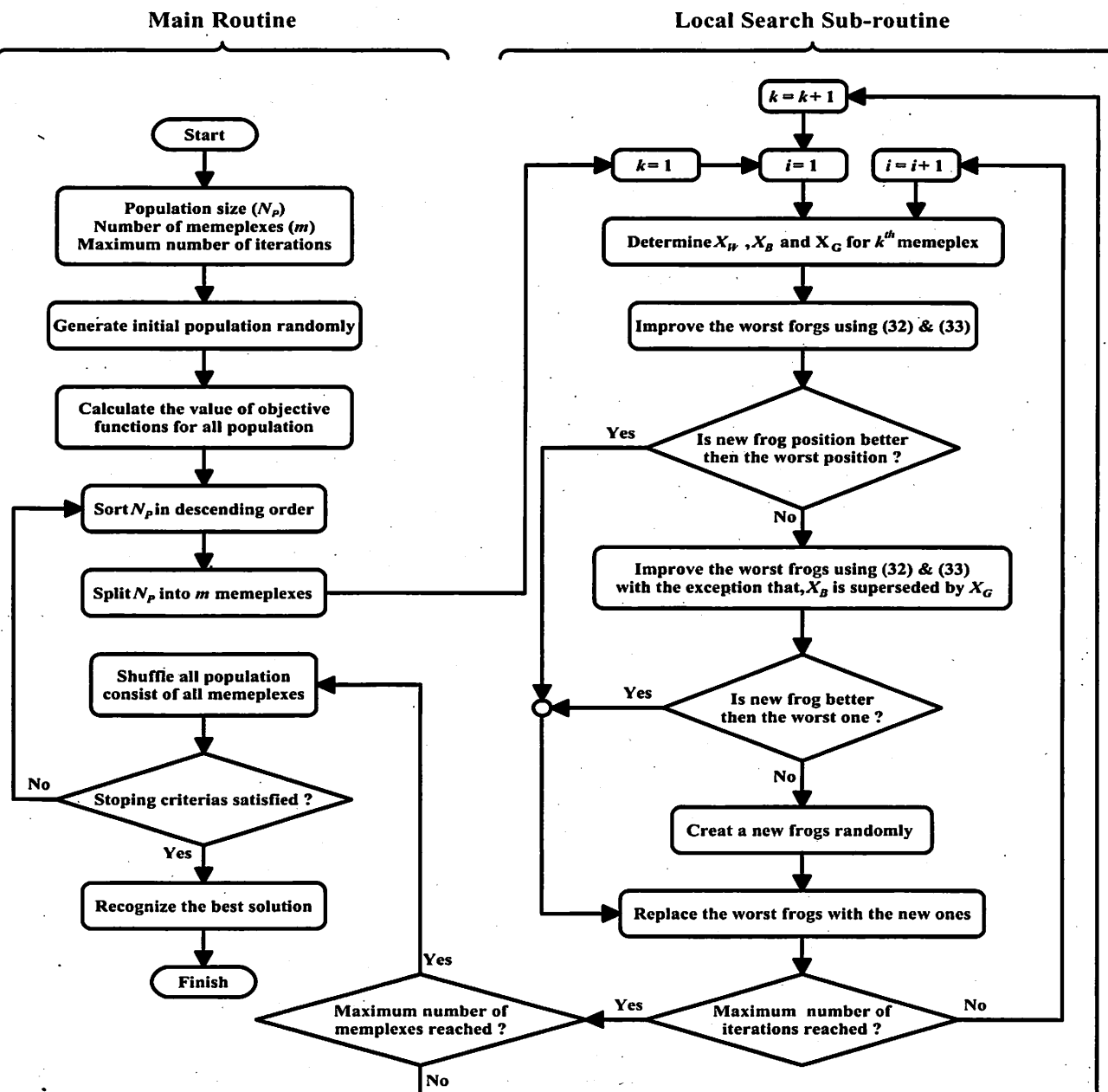


Fig. 6. The flowchart of SFLA including both main routine and local search.

may take place if (1) the population is trapped into local optima, (2) the population has lost its diversity. In order to ameliorate these issues a powerful mutation operator is proposed in this paper. The mechanism of the proposed mutation strategy is based on generating a trial mutant vector for improving the diversity of population. In this regard, (28) & (29) are applied for producing the mutant vector [41,42].

$$X_i^{\text{mutant}} = X_i^{\text{rand}} + \text{rand} \times (X_B^i - X_i^{\text{rand}}) + \text{rand} \times (X_G^i - X_i^{\text{rand}}) \quad (28)$$

$$i = 1, 2, \dots, m \quad (29)$$

Where,  $X_i^{\text{mutant}}$  is the mutant vector corresponding to mutation operator.  $X_i^{\text{rand}}$  is a randomly generated vector.  $\text{rand}$  is a random number between zero and one and  $m$  is the number of memplexes.

#### 4.3. Original PSO

PSO is an evolutionary-based optimization algorithm inspired by social manner of bird's migration and works based on probability laws [47]. In the PSO algorithm, at first a random population is generated and moving toward progress and updating their information. In this algorithm, each individual represent a possible solution and a sample solution is one particle in the search space and this particle has two important parameters including position and velocity. Along with running the algorithm, position and velocity of every particle are updated as follows [48]:

$$X_i^{t+1} = X_i^t + V_i^{t+1} \quad (30)$$

$$\begin{aligned} V_i^{t+1} = & \{w \times V_i^t\} + \left\{c_1 \times \text{rand} \times [P_{\text{Best},i}^t - X_i^t]\right\} + \left\{c_2 \times \text{rand}\right. \\ & \left. \times [G_{\text{Best}}^t - X_i^t]\right\} \end{aligned} \quad (31)$$

$$w = w_{\max} - \frac{(w_{\max} - w_{\min})}{\text{Iter}_{\max}} \times \text{Iter} \quad (32)$$

$$i = 1, 2, 3, \dots, N_p \quad (33)$$

Where,  $X_i^{t+1}$  and  $V_i^{t+1}$  are position and velocity of  $i$ th particle at  $(t+1)$ th iteration, respectively.  $X_i^t$  and  $V_i^t$  are position and velocity of  $i$ th particle at  $t$ th iteration, respectively.  $c_1$  and  $c_2$  are two positive constant bounded in range [1, 2] known as individual and social learning factors.  $\text{rand}$  is random number in range [0, 1].  $P_{\text{Best},i}^t$  is the best personal fitness value of  $i$ th particle at  $t$ th iteration.  $G_{\text{Best}}^t$  is the best value among all of  $P_{\text{Best},i}^t$  at  $t$ th iteration.  $N_p$  is populations size.  $\text{Iter}$  and  $\text{Iter}_{\max}$  are iteration and maximum number of iterations, respectively and finally,  $w$ ,  $w_{\min}$  and  $w_{\max}$  are inertia weight and its corresponding minimum and maximum boundaries, respectively.

#### 4.4. Hybrid MSFLA-PSO

In order to implement the proposed algorithm for solving the MODFR problem,  $(2 \times N_p)$  initial population are generated randomly and every EAs i.e. MSFLA and PSO algorithms starts its procedure by a  $N_p$  as size population. After each iteration, the best solutions obtained by algorithms are compared and the better one is used as the best solution for both EAs in the next iteration. The hybridization flowchart of MSFLA and PSO EAs is displayed in Fig. 7.

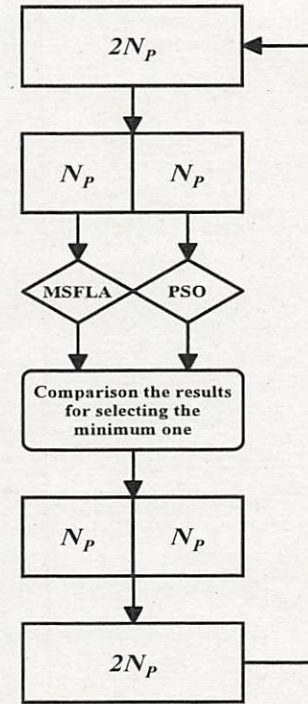


Fig. 7. Hybridization process of both MSFLA and PSO algorithms in this paper.

#### 5. Numerical and simulation outcomes

In order to evaluate the ability of the proposed algorithm, it is employed to optimize Schaffer's function and solve the DFR in two different and independent studies. It is worth mentioning that, all test cases are coded and performed in MATLAB environment on a quad-core processor laptop machine with 1.6 GHz clock frequency and 4.0 GB of RAM.

##### 5.1. Validation of proposed approach to minimize the Schaffer's function

This section illustrates the performance of HMSFLA-PSO for minimizing the Schaffer's function (a complicate function with several local optima) with two decision variables  $x_1$  and  $x_2$ . The Schaffer's function is a suitable test function to evaluate the ability of optimization algorithms since it has multiple local optima. The mathematic formula of this function is as follows [49,50]:

$$f(x) = 0.5 + \frac{\left(\sin \sqrt{x_1^2 + x_2^2}\right)^2 - 0.5}{(1 + 0.001 \times (x_1^2 + x_2^2))^2} \quad (41)$$

The 3-D and contour graphs of the Schaffer's function with two decision variables are depicted in Figs. 8 and 9, respectively. It is worth mentioning that, both decision variables  $x_1$  and  $x_2$  are bounded in  $[-10, +10]$ .

From Figs. 8 and 9, different regions from the worst region to the best one are shown using red, heavy yellow, light yellow and blue colors, respectively. In order to solve this problem, population size is set to 7 and maximum number of iterations are set to 30 and 15 for  $\text{Iter}_{\max}$  and  $\text{Iter}_{\min}$ , respectively. The optimal solution of the objective function is equal to 0 which occurs at (0, 0). The obtained results for initial and final iterations are depicted in Figs. 10 and 11 for the proposed algorithm and original PSO, respectively. It is

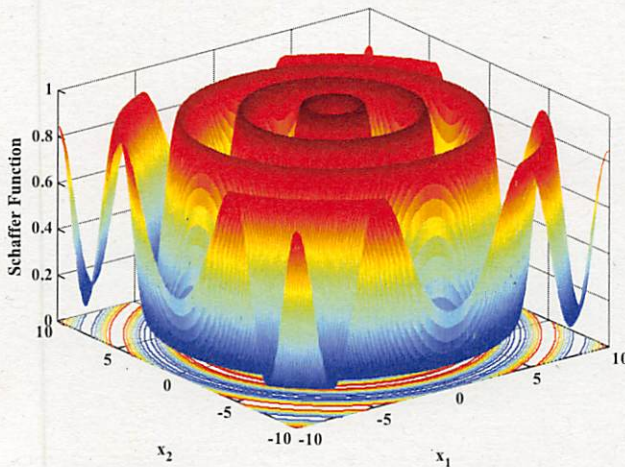


Fig. 8. 3-D plot of Schaffer's function with two decision variables.

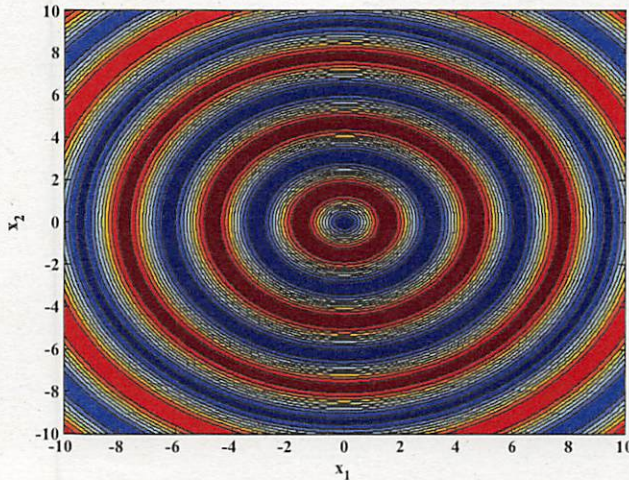


Fig. 9. Contour plot of Schaffer's function with two decision variables.

necessary to note that, the pentagrams which are illustrated in Figs. 10 and 11 are seven individuals in the search space of Schaffer's problem.

According to Figs. 10 and 11, the following points can be highlighted;

- In the original PSO algorithm six particles are trapped into local optimal points. It is the prominent drawback of this algorithm.
- All particles in the proposed HMSFLA-PSO algorithm find the global optimal solution of Schaffer' problem.
- Finding the global optimal solution by HMSFLA-PSO approves the performance and search ability of the proposed algorithm for optimizing complex multimodal benchmark functions such as Schaffer's problem.

## 5.2. Substrate preparation to solve the proposed DFR problem in this paper

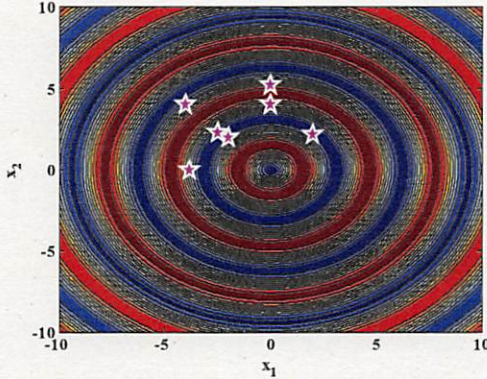
In this section, a MATLAB code is written in MATLAB R2014a environment for the HMSFLA-PSO algorithm, BFS (for power flow procedure in distribution systems), and proposed objective functions. The proposed algorithm has several essential parameters which must be set initially in order to solve the DFR and MODFR problems. To this end, Table 3 tabulates these important and effective parameters and intervals for the HMSFLA-PSO algorithm which are obtained based on several trials and errors.

### 5.2.1. Test systems

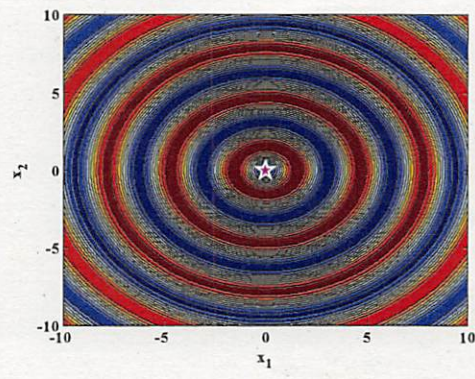
In this section, two different employed test systems including IEEE 33-node and 95-node distribution networks are presented.

**5.2.1.1. Test system 1 (IEEE 33-node distribution network).** The IEEE 33-node distribution system consists of four 500 KW DG units which are located at nodes #6, #12, #16 and #31. The electricity cost of sub-station is 0.04 \$/KWh and the related costs of DG units are 0.043 \$/KWh, 0.042 \$/KWh, 0.042 \$/KWh and 0.043 \$/KWh for DGs installed at nodes #6, #12, #16 and #31, respectively. The cost of switching is 0.041 \$/Switching [1]. The single-line diagram of test system 1 is displayed in Fig. 12. The rest of essential information for this test system is provided in Appendix A (Tables A1–A3).

**5.2.1.2. Test system 2 (IEEE 95-node distribution network).** The IEEE 95-node is a relatively large-scale distribution system includes nine DG units with 1 MW capacity which are located at nodes #6, #10, #20, #25, #34, #41, #50, #70, and #76. The cost of sub-station is 0.041 \$/KWh and the related costs of DG units are 0.042 \$/KWh for all DG units. The cost of switching is 0.041 \$/Switching. The single-



(a) After first iteration



(b) After final iteration

Fig. 10. Obtained results from HMSFLA-PSO for minimizing the Schaffer's function. (a) After the initial iteration, (b) After the final iteration.

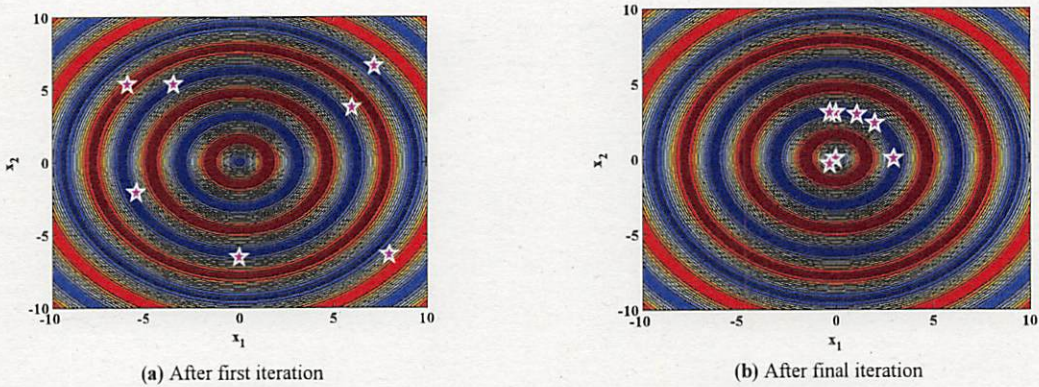


Fig. 11. Obtained results from original PSO for minimizing the Schaffer's function (a) After the initial iteration, (b) After the final iteration

**Table 3**  
Descriptions of important parameters of the proposed algorithm.

Essential Parameters and intervals	Proposed HMSFLA-PSO
$N_p$	300
$n$	30
$m$	10
$\widehat{iter}_{max}$	100
$\widehat{\widehat{iter}}_{max}$	40
$w$	[0.4 – 0.9]
$c_1$	1.49618
$c_2$	1.49618

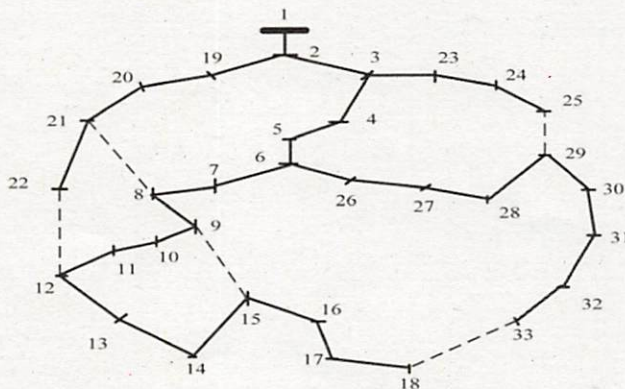


Fig. 12. Single-line diagram of IEEE 33-node distribution test system.

line diagram of test system 2 is displayed in Fig. 13. More information about this system can be found in Ref. [51].

Different studies in DFR area consider different test systems with various locations and sizes for distributed generations. Toward this end a comparison is presented for IEEE 39-bus test systems with/out DG in order to prove the ability of the proposed algorithm in solving complex optimization problems. Obtained results for loss objective function juxtaposed with corresponding control variables are shown in Tables 4 and 5 for IEEE 39-bus test systems with/out DG, respectively. Table 4 includes best, mean, worst and Standard Deviation (STD) for 10 independent trials. It is clear that the proposed algorithm has obtained the best solution and also has the lowest standard deviation which prove the ability of the propose algorithm in converging to global optima in different trials. Table 5 provides the best obtained solution and corresponding control variables for different optimization algorithms in which all of them

are coded by authors. From this table it is clear that, the proposed algorithm is superior in finding the best optimal solution.

### 5.2.2. Case studies

Different scenarios for each test system are modeled and investigated to distinguish the characteristic of each objective function in the proposed problem. These scenarios are tabulated in Table 6.

According to Table 6, for both test systems at first every objective function is minimized individually to find out the extreme points of trade-off curve and calculate the  $f_i^{min}$  and  $f_i^{max}$  values for  $i^{th}$  objective function which  $i = 1, 2, 3$ . These extreme point are useful for finding the Pareto-fronts in multi-objective cases.

**5.2.2.1. IEEE 33-node test system.** This sub-section investigates all three objective functions in 33-node distribution system in order to demonstrate the performance of the proposed algorithm in solving the DFR problem. The obtained results are tabulated in Tables 7 and 8 for Cases 1–3 in which Table 7 presents the numerical values of all three objective functions and Table 8 tabulates the control variables. It is notable that, the results of interest are **bold faced** for each objective function in Table 7. It is necessary to note that the optimal value for switching objective function is zero, which implies no change in the network configuration.

One of the main goals of the proposed approach is solving the proposed DFR problem as a MOOP. In this regard, the obtained results for solving Cases 4–7 (MOOP cases) are presented in Tables 9–12, respectively where, the Best Compromise Solution (BCS) for each case is shown and compared with those obtained by PSO and DE algorithms. From these tables it is clear that, the BCS obtained by the proposed algorithm dominates those obtained by other evolutionary algorithms. Another advantage of the proposed algorithm is obtaining different optimal points for the proposed problem when it is solving as MOOP. Having different choices that satisfied our purpose could help to select one desirable choice among them. In this regard, Pareto-optimal solution which can obtain a squad of results is a very significant and acceptable method for solving the MOOP. That is why the Pareto-optimal solution method is applied to solve the proposed problem. The Distribution System Operator (DSO) can select one of the solutions tabulate in Table 9, based on his/her desire. Same story is valid for choosing the desired solution for other cases i.e. Tables 10–12

Furthermore, all two- & three-dimensional Pareto-optimal solutions are illustrated in Fig. 14. In this regard, the two-dimensional Pareto-optimal fronts related to propose DFR problem are displayed in parts (a) to (c). Furthermore, part (d) demonstrates the three-dimensional Pareto-optimal solutions. These figures can

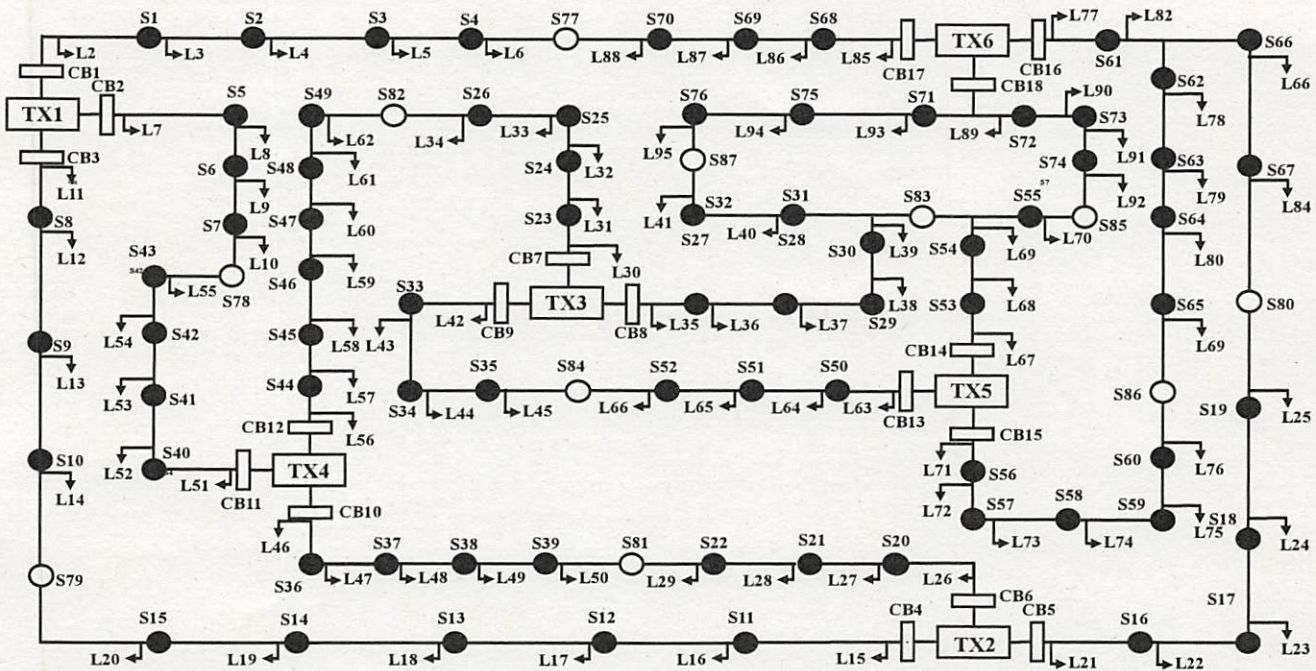


Fig. 13. Single-line diagram of IEEE 95-node distribution test system.

**Table 4**

Power loss for 33-bus test system without considering DG units.

Algorithms	Variation Parameters of best solution					Power loss (KW)				
	Sw1	Sw2	Sw3	Sw4	Sw5	Best	Mean	Worst	STD	Time (s)
McDermott et al. [52]	37	32	14	9	7	139.53	—	—	—	1.99
DPSO-ACO [53]	37	32	14	9	7	139.53	—	—	—	~8
Shirmohammadi and Hong [53]	37	32	14	10	7	140.26	—	—	—	0.14
HBMO [54]	37	32	14	9	7	139.53	—	—	—	~8
GA	37	34	30	9	7	140.282	141.690	143.940	1.431	27.43
PSO	37	30	14	19	7	139.982	140.230	141.921	0.605	18.32
Proposed Algorithm	37	32	14	9	7	139.530	139.530	139.530	0	6.73

**Table 5**

Power loss for 33-bus test system considering DG units.

Algorithms	Variation Parameters of best solution									Power loss (KW)			
	Sw1	Sw2	Sw3	Sw4	Sw5	Bus#6	Bus#12	Bus#16	Bus#31	Best	Mean	Worst	STD
GA	33	14	9	32	28	499.5	449.5	300.0	449.5	76.9914	79.65905	84.7922	3.5507
PSO	33	14	9	32	28	499.5	499.5	400.5	499.5	71.6689	75.0476	79.2377	3.9572
TLBO	33	14	9	32	28	499.5	499.5	449.5	499.5	70.5079	71.1247	71.5138	0.4862
Proposed Algorithm	33	14	9	32	28	499.5	499.5	499.5	499.5	69.396294	70.326349	70.9633	0.6623

**Table 6**

Description of various case studies in this paper.

Scenarios	Objective functions			Test system			
	Power loss	VSI	Switching				
Case 1	✓	—	—	Both IEEE 33- and 95-node test systems			
Case 2	—	✓	—				
Case 3	—	—	✓				
Case 4	✓	✓	—				
Case 5	✓	—	✓				
Case 6	—	✓	✓				
Case 7	✓	✓	✓				

**Table 7**

Best obtained results for different objective functions for Cases 1–3 on test system 1.

Objective functions	Power loss (KW)	VSI	Switching
Power Loss (KW)	<b>69.39629413</b>	Unstable (above 1)	4
VSI	145.1315444	<b>0.659958918</b>	4

discovered without the proposed multi-objective optimization algorithm. It is worth mentioning that the BCSs can be obtained by applying (22). The system operator can change the importance factor of different objective functions according to his/her decision. In this regard, if one objective is more important than others, the

**Table 8**

DGs output and switches for Cases 1–3 on test system 1.

Control Variables		Power loss (KW)	VSI	Switching
Switches	Sw <sub>1</sub>	33	6	33
	Sw <sub>2</sub>	14	11	34
	Sw <sub>3</sub>	9	8	35
	Sw <sub>4</sub>	32	31	36
	Sw <sub>5</sub>	28	37	37
Output of DG units	Bus#6	499.5	100	—
	Bus#12	499.5	100	—
	Bus#16	499.5	100	—
	Bus#31	499.5	200	—

**Table 9**

Obtained results and decision variables for Case 4 on test system 1.

Algorithms	Switches					DG units				Objective functions	
	Sw1	Sw2	Sw3	Sw4	Sw5	DG1	DG2	DG3	DG4	Power loss (KW)	VSI
Proposed Algorithm	33	14	9	32	28	357	466	357	404	78.2160	0.9044
PSO	33	13	9	32	28	391	474	380.5	431.5	79.7591	0.9263
DE	33	14	9	31	28	417	481.5	332	455	82.0994	0.9096

**Table 10**

Obtained results and decision variables for Case 5 on test system 1.

Algorithms	Switches					DG units				Objective functions	
	Sw1	Sw2	Sw3	Sw4	Sw5	DG1	DG2	DG3	DG4	Power loss (KW)	Switching
Proposed Algorithm	6	34	9	36	37	339	454.5	489.5	500	80.8665	2
PSO	6	34	9	36	37	365	431	498	487	81.4779	2
DE	6	34	9	36	37	340.5	355	499	499.5	83.5660	2

**Table 11**

Obtained results and decision variables for Case 6 on test system 1.

Algorithms	Switches					DG units				Objective functions	
	Sw1	Sw2	Sw3	Sw4	Sw5	DG1	DG2	DG3	DG4	VSI	Switching
Proposed Algorithm	6	11	35	36	37	100	100	100	204.5	0.6964	2
PSO	6	11	35	36	37	104.5	114.5	200	194.5	0.7163	2
DE	6	11	35	36	37	242.5	100	100	200	0.7186	2

**Table 12**

Obtained results and decision variables for Case 7 on test system 1.

Algorithms	Switches					DG units				Objective functions	
	Sw1	Sw2	Sw3	Sw4	Sw5	DG1	DG2	DG3	DG4	VSI	Switching
Proposed Algorithm	6	11	35	36	37	100	186.5	151	154.5	127.4194	0.7225
PSO	6	13	35	36	37	103.5	154.5	150	154	127.4703	0.7277
DE	6	13	35	36	37	119.5	114.5	104.5	135	132.5811	0.7059

approve the ability of the HMSFLA-PSO algorithm for solving the proposed MODFR problem in both 2-D and 3-D forms.

From Fig. 14, it is clear that the best obtained value for each objective function in all Pareto-fronts is very close to its corresponding optimized value while the objective is optimized, individually. Such important optimal solutions could not have

DSO can increase its corresponding importance factor. Therefore this process helps the DSO have extensive choices.

In order to demonstrate the searching ability of the proposed algorithm, we run the proposed algorithm 50 times for test system 1. The obtained values of best, average, worst, and standard deviation are tabulated in Table 13 for 50 independent trials.

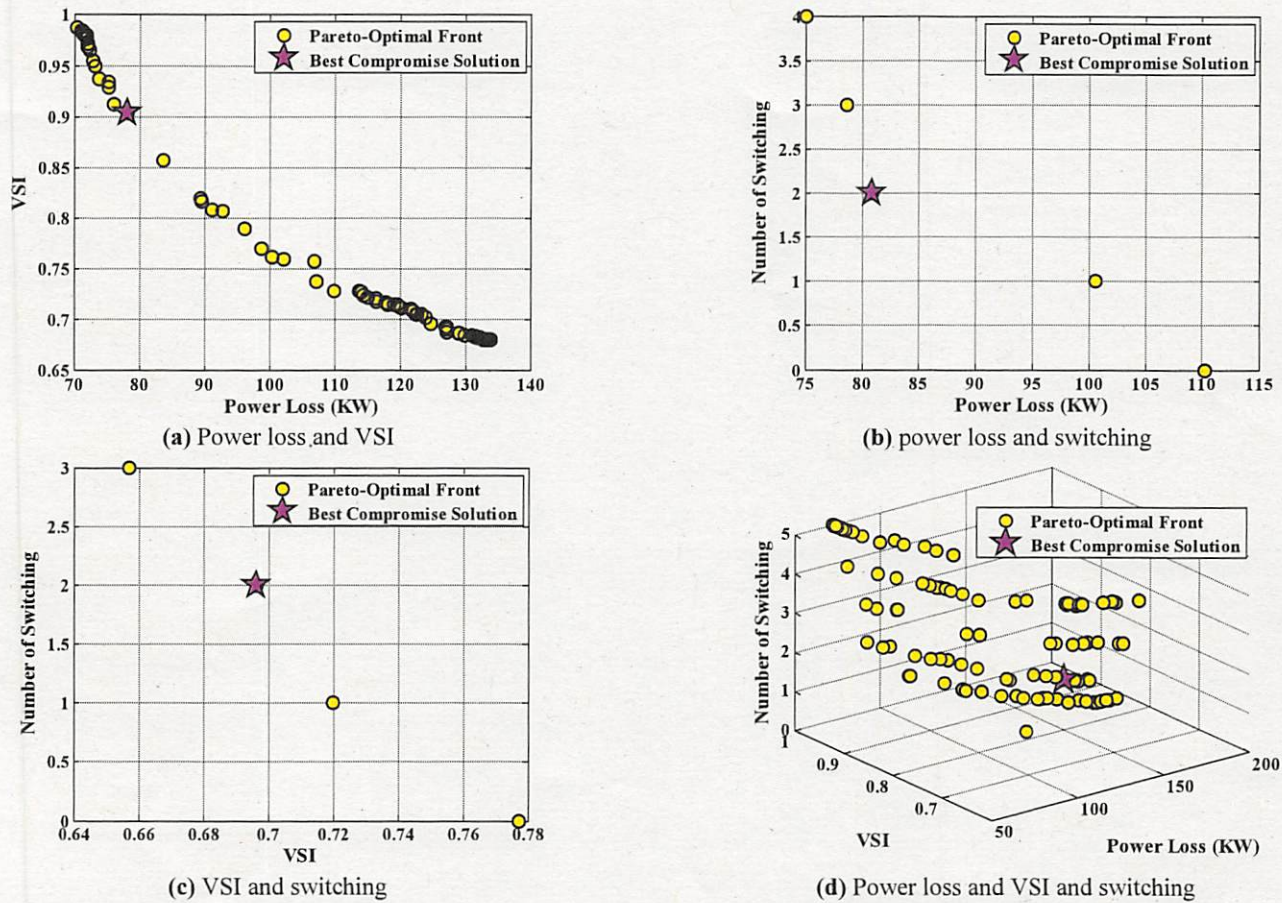


**Fig. 14.** Best obtained two-and three-dimension Pareto-fronts from proposed algorithm on test system 1 for (a)Power loss and VSI, (b) power loss and switching, (c) VSI and switching and (d) all three objectives

**Table 13**  
Obtained results by the proposed algorithm for 50 independent runs.

Objective functions	Best solution	Average Value	Worst solution	Standard deviation
Power Loss (MW)	69.39629	70.7889	72.8778	1.7978
VSI	0.659959	0.6754	0.69384	0.0162

According to **Table 13**, the value of standard deviation for both objective functions verifies the performance of the HMSFLA-PSO algorithm for solving the DFR problem with different objectives.

**5.2.2.2. IEEE 95-node test system.** The proposed algorithm is employed to solve the DFR problem in 95-node test systems in order to evaluate the performance of the proposed algorithm in solving single and multi-objective DFR problems in large scale test system. The best obtained results for each objective function for Cases 1–3 are tabulated in **Table 14**. It is notable that, the results of interest are **bold faced** for each objective function in **Table 14**. Furthermore, the corresponding decision variables for these cases

are tabulated in **Table 15**.

The obtained results for solving Cases 4–7 on test system 2 are tabulated in **Tables 16–23**. DGs output and switch statuses for Case 4 are tabulated in **Tables 16 and 17**, respectively. It is notable that, the corresponding objective functions value for Case 4 are shown in **Table 16** along with the DGs output. In order to prove the ability of the proposed algorithm in solving the MOOP, the obtained BCS is compared with those obtained by PSO and DE algorithms. From this comparison it is evident that, the obtained result by proposed algorithm dominates those obtained by PSO and DE algorithms which proves the ability of the proposed algorithm. **Tables 18 and 19** tabulate the obtained results for Case 5, in which the output of DG units and values of objective functions are depicted in **Table 18** while **Table 19** presents the corresponds switches status. Similarly **Tables 20 and 21** and also 22 & 23 depict the obtained results for Cases 6 & 7 respectively. The obtained results in each case are compared with those obtained by PSO and DE algorithms. These comparison shows the supremacy of the proposed algorithm in solving single- and multi-objective optimization problem.

**Table 14**  
Best solution obtained by the proposed algorithm for Cases 1–3 on test system 2.

Objective functions	Power loss (MW)	VSI	Switching
Power Loss (MW)	<b>449.9071627</b>	0.12588663	7
VSI	645.081	<b>0.05337</b>	4

**Table 15**  
Decision variables for Cases 1–3 on test system 2.

Control Variables		Power loss (MW)	VSI	Switching
Switches	<i>Sw</i> <sub>1</sub>	77	3	77
	<i>Sw</i> <sub>2</sub>	43	78	78
	<i>Sw</i> <sub>3</sub>	15	79	79
	<i>Sw</i> <sub>4</sub>	39	21	80
	<i>Sw</i> <sub>5</sub>	82	82	81
	<i>Sw</i> <sub>6</sub>	35	35	82
	<i>Sw</i> <sub>7</sub>	67	19	83
	<i>Sw</i> <sub>8</sub>	65	86	84
	<i>Sw</i> <sub>9</sub>	85	85	85
	<i>Sw</i> <sub>10</sub>	87	87	86
	<i>Sw</i> <sub>11</sub>	30	83	87
Output of DG units	Bus#6	1000	755	—
	Bus#10	1000	380	—
	Bus#20	1000	960	—
	Bus#25	1000	730	—
	Bus#34	1000	600	—
	Bus#41	1000	710	—
	Bus#50	1000	660	—
	Bus#70	1000	960	—
	Bus#76	1000	230	—

**Table 16**  
DGs output and values of objective functions for solving Case 4 on test system 2.

Algorithms	Output of DG units									Objective functions	
	DG1	DG2	DG3	DG4	DG5	DG6	DG7	DG8	DG9	Power loss (KW)	VSI
Proposed Algorithm	965	220	935	915	785	925	520	955	95	594.3737	0.0660
PSO	875	220	555	875	385	915	500	910	125	605.9850	0.0711
DE	860	300	875	735	430	415	625	825	100	614.7896	0.0696

**Table 17**  
Switches for solving Case 4 on test system 2.

Algorithms	Switches										
	Sw1	Sw2	Sw3	Sw4	Sw5	Sw6	Sw7	Sw8	Sw9	Sw10	Sw11
Proposed Algorithm	4	78	79	22	82	35	19	86	85	87	83
PSO	4	78	79	22	82	35	19	86	85	87	83
DE	4	78	79	22	82	35	19	86	85	87	83

**Table 18**  
DGs output and values of objective functions for solving Case 5 on test system 2.

Algorithms	Output of DG units									Objective functions	
	DG1	DG2	DG3	DG4	DG5	DG6	DG7	DG8	DG9	Power loss (KW)	Switching
Proposed Algorithm	990	990	990	990	990	990	990	990	990	536.3748	4
PSO	775	1000	990	990	1000	1000	1000	890	1000	574.8995	5
DE	1000	1000	990	990	1000	1000	1000	1000	1000	574.5602	5

**Table 19**  
Switches for solving Case 5 on test system 2.

Algorithms	Switches										
	Sw1	Sw2	Sw3	Sw4	Sw5	Sw6	Sw7	Sw8	Sw9	Sw10	Sw11
Proposed Algorithm	4	43	15	81	82	84	80	86	55	87	83
PSO	3	43	15	81	82	84	80	86	55	87	83
DE	3	43	15	81	82	84	80	86	55	87	54

From Tables related to MOOP, it is clear that the proposed algorithm can handle the MOOP irrespective of their complexities and number of objective functions. In addition, all two- and three-dimensional Pareto-optimal fronts for test system 2 are displayed in Fig. 15.

According to Figs. 14 and 15 it is clear that, the proposed hybrid algorithm can handle MOOPs irrespective of their size and complexities. It is shown vividly, in all Pareto-front figures, that the proposed algorithm can find several non-dominated solutions for each case. It is notable having discrete decision variable in

**Table 20**

DGs output and values of objective functions for solving Case 6 on test system 2.

Algorithms	Output of DG units									Objective functions	
	DG1	DG2	DG3	DG4	DG5	DG6	DG7	DG8	DG9	VSI	Switching
Proposed Algorithm	1000	1000	1000	230	1000	1000	1000	1000	1000	0.1264	4
PSO	985	1000	1000	270	1000	1000	999	999	1000	0.1276	4
DE	985	1000	989	420	1000	1000	999	1000	1000	0.1266	4

**Table 21**

Switches for solving Case 6 on test system 2.

Algorithms	Switches										
	Sw1	Sw2	Sw3	Sw4	Sw5	Sw6	Sw7	Sw8	Sw9	Sw10	Sw11
Proposed Algorithm	77	43	15	81	82	84	80	86	55	87	30
PSO	77	43	14	81	82	84	80	86	55	87	29
DE	77	43	15	81	82	84	80	86	55	87	29

**Table 22**

DGs output and values of objective functions for solving Case 7 on test system 2.

Algorithms	Output of DG units									Objective functions		
	DG1	DG2	DG3	DG4	DG5	DG6	DG7	DG8	DG9	Power loss (KW)	VSI	Switching
Proposed Algorithm	985	995	915	835	975	960	995	980	970	502.5196	0.1326	4
PSO	1000	995	925	999	1000	1000	995	999	1000	515.8979	0.1333	4
DE	1000	999	999	1000	1000	1000	1000	995	1000	0.534301	0.1325	5

**Table 23**

Switches for solving Case 7 on test system 2.

Algorithms	Switches										
	Sw1	Sw2	Sw3	Sw4	Sw5	Sw6	Sw7	Sw8	Sw9	Sw10	Sw11
Proposed Algorithm	77	43	79	81	82	35	19	86	85	32	83
PSO	77	43	79	81	82	35	17	86	85	31	83
DE	69	43	79	81	82	35	19	86	85	31	83

optimization problem usually leads to discontinuity in Pareto-fronts which is clear in all obtained Pareto-fronts. It is clear the DSO has different choices for operating the distribution system in which s/he can select one based on her/his desire in different condition.

### 5.2.3. Analysis of pareto-optimal solutions

One of the main targets of this study is solving the DFR problem as MOOP. Therefore it is too important to implement some measures to authenticate the obtained Pareto-optimal solutions. To this end, three different measures are implemented to authenticate the suitability of obtained Pareto-optimal fronts.

**5.2.3.1. Generational distance.** Generational Distance (GD) criterion is best candidate to find how far each solution is in the set of non-dominated solutions. The GD criterion can be modeled as follows [55]:

$$GD = \sqrt{\frac{\sum_{k=1}^K EGD_k^2}{K}} \quad (42)$$

Where  $EGD_k$  is the Euclidean geometrical distance between every of vectors i.e. non-dominated solutions, and the closest number of Pareto-optimal collection. To this end, it is necessary to note that the zero value for GD demonstrates that all of generated components are in Pareto-optimal collection. Therefore a less value for GD parameter is more desirable.

**5.2.3.2. Spacing parameter.** The Spacing Parameter (SP) criterion is another important parameter to analyze the Pareto-optimal solutions which can be defined as a distribution of these solutions in the Pareto-fronts [42]. The SP criterion is presented in (43)–(45) as variance of neighboring vectors in the non-dominated solutions.

$$SP = \sqrt{\frac{1}{m-1} \sum_{y=1}^Y (dis - dis_y)^2} \quad (43)$$

$$dis_y = \min \left( |F_1^y(X) - \hat{F}_1^y(X)| + |F_2^y(X) - \hat{F}_2^y(X)| + \dots + |F_{N_{obj}}^y(X) - \hat{F}_{N_{obj}}^y(X)| \right) \quad (44)$$

$$y, \hat{y} = 1, 2, \dots, Y \quad (45)$$

Where,  $dis$  is the average of all  $dis_y$ .

It is notable that, the zero value for SP illustrates all members of achieved Pareto-front are spaced as equidistantly. Therefore a less value for SP parameter is more valuable.

**5.2.3.3. Diversity metric.** The final criterion to analyze the obtained Pareto-optimal solutions is Diversity Metric (DM). This factor is based on the geometrical distance of Euclidean and Hamming

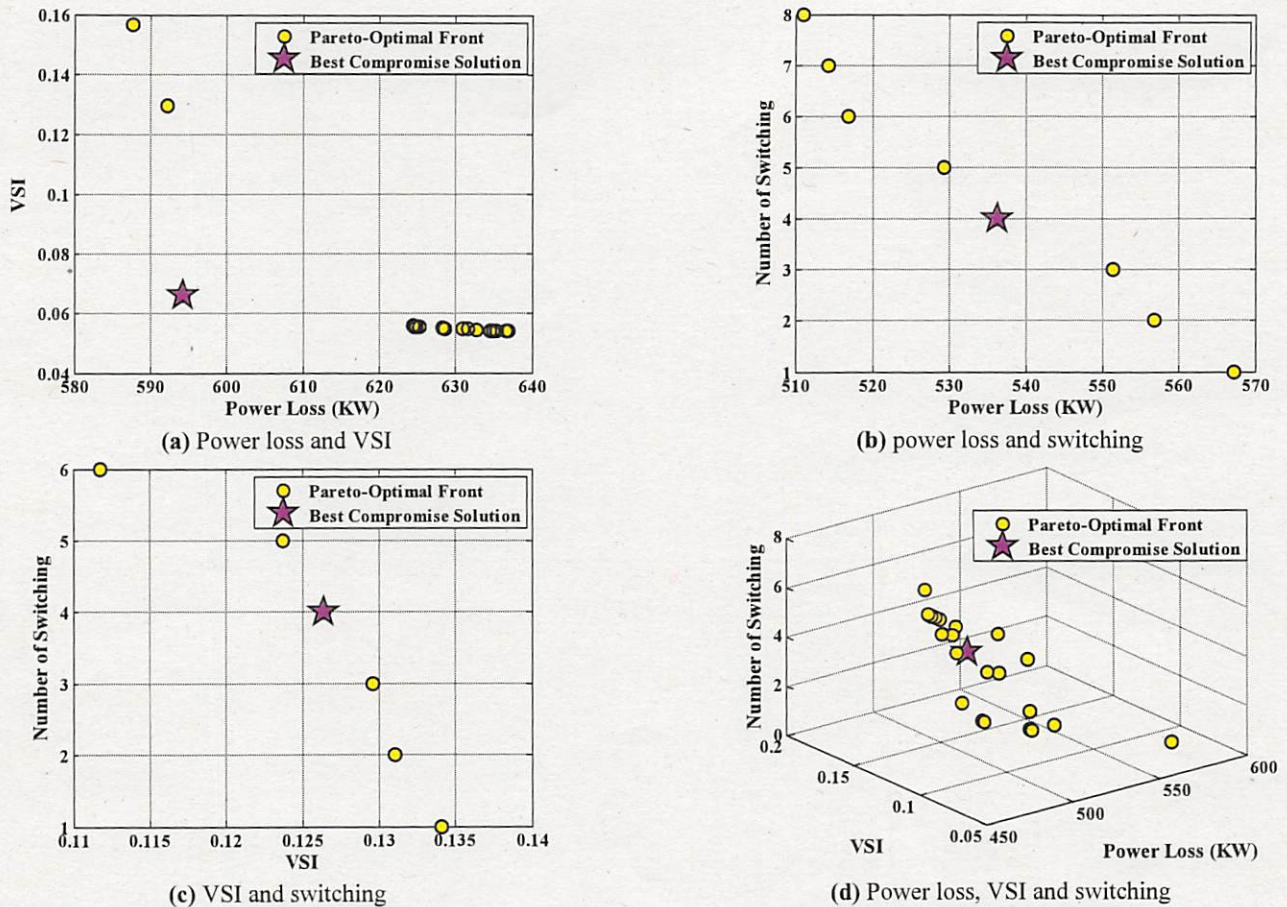


**Fig. 15.** Best obtained two-and three-dimension Pareto-fronts from proposed algorithm on test system 2 for. (a) Power loss and VSI, (b) power loss and switching, (c) VSI and switching and (d) all three objectives

between obtained Pareto-solutions [42]. Toward this end, if there is  $m$  number of points in the Pareto-front with  $N_{OF}$  dimensional space, the centroid for  $n$ th dimension is presented as follows;

$$C_n = \frac{\sum_{l=1}^L \dim_{nl}}{m} \quad (46)$$

$$n = 1, 2, \dots, N_{OF} \quad (47)$$

Where,  $\dim_{nl}$  is  $n$ th dimension of the  $l$ th point and  $C_n$  is centroid point for  $n$ th dimension and based on (46) & (47), the formulation for DM is as follows;

$$DM = \sum_{n=1}^{N_{OF}} \sum_{l=1}^L (\dim_{nl} - C_n)^2 \quad (48)$$

It is noteworthy that, the greater value for DM indicates that all of generated arrays are close to each other.

The obtained best values of GD, SP and DM criterions in both two- and three-dimensional Pareto-fronts related to MODFR problem are tabulated in Table 24, which are achieved by the proposed HMSFLA-PSO algorithm.

According to Table 24, it is obvious that the proposed algorithm is able to handle MOOPs very well. Therefore, the ability of the proposed HMSFLA-PSO algorithm for solving the MODFR problem is proven once again.

**Table 24**

Best GD, SP and DM for Pareto-optimal solutions obtained by the proposed algorithm.

Test systems	Dimensional of problem	Criterions	HMSFLA-PSO
Test system 1	Power loss and VSI	GD	0.1828
		SP	1.0066
		DM	39101.89
	Power loss and switching	GD	1.6455
		SP	3.8572
		DM	963.5268
	VSI and switching	GD	0.5004
		SP	0.0161
		DM	5.0076
	Power loss and VSI and switching	GD	0.1136
		SP	0.9556
		DM	85738.36
Test system 2	Power loss and VSI	GD	0.3414
		SP	1.1608
		DM	4113.648
	Power loss and switching	GD	2.1599
		SP	2.6198
		DM	3191.362
	VSI and switching	GD	0.4084
		SP	0.0041
		DM	17.5003
	Power loss and VSI and switching	GD	0.5802
		SP	3.0304
		DM	21761.15

## 6. Conclusions

A novel hybrid evolutionary algorithm has been successfully implemented in this paper to solve single- and multi-objective versions of Distribution Feeder Reconfiguration (DFR) problem. Stability challenges emerged by increasing penetration level of Renewable Energy Sources (RES) in distribution systems which has been neglected in most studies is investigated in this paper. A voltage stability index related to the short circuit capacity of the system is considered as an objective function beside the conventional objective functions i.e. power losses and number of switching. A Pareto-optimal solution based on the dominance concept is employed to solve the presented multi-objective optimization problem. The proposed Hybrid Modified Shuffled frog Leaping Algorithm-Particle Swarm Optimization (HMSFLA-PSO) has been applied on two different test system including small-and large-scale distribution networks such as IEEE 33- and 95-node test systems. Furthermore the proposed approach is applied on different case studies in order to scrutinize the effect of DFR on each objective function. Yet another, three criterions are implemented to evaluate the quality of the Pareto-optimal solutions obtained by the proposed algorithm. Finally, the following conclusions can be outlined;

- The proposed hybrid optimization algorithm has a stable performance for solving the DFR problem in both small- and large-scale distribution networks.
- The proposed algorithm can handle both single- and multi-objective optimization problems irrespective of their complexity and scales.
- Impacts of DFR on voltage stability enhancement in the form of VSI are investigated in this study.
- The proposed algorithm is capable of finding well-distributed Pareto-front for all MOOPs.

## Appendix A. Data for test system 1 (IEEE 33-node distribution network)

**Table A2**  
Branches data

Branch number	From node	To node	R(Ω)	X(Ω)
1	1	2	0.0922	0.0470
2	2	3	0.4930	0.2512
3	3	4	0.3661	0.1864
4	4	5	0.3811	0.1941
5	5	6	0.8190	0.7070
6	6	7	0.1872	0.6188
7	7	8	0.7115	0.2351
8	8	9	1.0299	0.7400
9	9	10	1.0440	0.7400
10	10	11	0.1967	0.0651
11	11	12	0.3744	0.1298
12	12	13	1.4680	1.1549
13	13	14	0.5416	0.7129
14	14	15	0.5909	0.5260
15	15	16	0.7462	0.5449
16	16	17	1.2889	1.7210
17	17	18	0.7320	0.5739
18	2	19	0.1640	0.1565
19	19	20	1.5042	1.3555
20	20	21	0.4095	0.4784
21	21	22	0.7089	0.9373
22	3	23	0.4512	0.3084
23	23	24	0.8980	0.7091
24	24	25	0.8959	0.7071
25	6	26	0.2031	0.1034
26	26	27	0.2842	0.1447
27	27	28	1.0589	0.9338
28	28	29	0.8043	0.7006
29	29	30	0.5074	0.2585
30	30	31	0.9745	0.9629
31	31	32	0.3105	0.3619
32	32	33	0.3411	0.5302

**Table A3**  
The data for tie-switches

Tie-switch number	From node	To node	R	X
33	8	21	2.0000	2.0000
34	9	15	2.0000	2.0000
35	12	22	2.0000	2.0000
36	18	33	0.5000	0.5000
37	25	29	0.5000	0.5000

**Table A1**  
Data for power nodes

Node number	Active power (KW)	Reactive power (KVAR)	Node number	Active power (KW)	Reactive power (KVAR)
1	100.00	60.00	17	90.00	40.00
2	90.00	40.00	18	90.00	40.00
3	120.00	80.00	19	90.00	40.00
4	60.00	30.00	20	90.00	40.00
5	60.00	20.00	21	90.00	40.00
6	200.00	100.00	22	90.00	50.00
7	200.00	100.00	23	420.00	200.00
8	60.00	20.00	24	420.00	200.00
9	60.00	20.00	25	60.00	25.00
10	45.00	30.00	26	60.00	25.00
11	60.00	35.00	27	60.00	20.00
12	60.00	35.00	28	120.00	70.00
13	20.00	80.00	29	200.00	600.00
14	60.00	10.00	30	150.00	70.00
15	60.00	20.00	31	210.00	100.00
16	60.00	20.00	32	60.00	40.00

## References